ative excess of pyrimidines over purines in the third position. The expected distribution in that case does not, however, match the observed distribution very well ($\chi_1^2 = 7.7$, $P < .01$). Thus secondary structure is unlikely to be the principal determinant of the observed bias.

One remaining possibility is that the frequency of purines and pyrimidines in the fourfold degenerate codons is necessarily positively correlated to the frequency of amino acids whose third codon position is necessarily a purine or pyrimidine. This could presumably arise through a kind of equilibrium between those amino acids that must be coded by third-position purines or pyrimidines and those that are indifferent to the nature of the third nucleotide. There are 235 pyrimidine restricted codons in MS2 phage and 169 purine restricted codons (the numbers do not include tryptophan, methionine, or isoleucine codons). Thus 0.582 of the restricted codons are pyrimidine restricted, and 0.582 of 565 fourfold degenerate codons is 328.7 codons—a value not significantly different from, indeed it is remarkably close to, the 326 actually observed. One cannot, however, prove a null hypothesis statistically. Failure to reject may simply mean that the sample size was too small or the test too ill-suited to discriminate among alternatives. Moreover, there is no reason why, if the basic concept is correct, all four nucleotides individually ought not to display a similar distribution in the two classes of codons, restricted and fourfold degenerate. Since there is, among fourfold degenerate codons ending in pyrimidine, a 10 percent excess of U over C in the third position (171 as compared to 155) these two nucleotides vary significantly in frequency from that expected on the basis of their frequency in the pyrimidine restricted codons.

WALTER M. FITCH
Department of Physiological Chemistry, University of Wisconsin, Madison 53706

References and Notes

1. F. H. C. Crick, *J. Mol. Biol.* **19**, 548 (1966).
2. B. G. Barrell and B. F. C. Clark, *Handbook of Nucleic Acid Sequences* (MRC Laboratory of Molecular Biology, Cambridge, England, 1974); G. A. Everett and J. T. Madison, *Biochemistry* **15**, 1016 (1976); C. Guerrier-Takada, G. Dirheimer, H. Grosjean, G. Keith, *FEBS Lett.* **60**, 286 (1975); N. J. Holness and G. Atfield, *Biochem. J.* **153**, 447 (1976).
3. The abbreviations for the amino acids in the order mentioned are Asn, asparagine; Ser, serine; His, histidine; Asp, aspartic acid; Tyr, tyrosine; Cys, half-cystine; Phe, phenylalanine; Ala, alanine; Pro, proline; Gly, glycine; and Val, valine.
4. W. Fiers, R. Contreras, F. Duerink, G. Haegeman, J. Merregaert, W. Min Jou, A. Raeymakers, G. Volchaert, M. Ysebaert, *Nature (London)* **256**, 273 (1975); W. Min Jou, G. Haegeman, M. Ysebaert, W. Fiers, *ibid.* **237**, 82 (1972); W. Fiers *et al.*, *ibid.* **260**, 500 (1976).
5. Supported by NSF grant BMS 75-20109.

7 June 1976; revised 3 September 1976

Bone Compressive Strength: The Influence of Density and Strain Rate

Abstract. *The compressive strength of bone is proportional to the square of the apparent density and to the strain rate raised to the 0.06 power. This relationship is applicable to trabecular and compact bone, and provides clinical guidelines for predicting bone strength on the basis of x-ray and densitometric examination.*

A typical long bone is composed of bone tissue in two forms of structural organization. Compact bone forms the cortex of the central shaft (diaphysis) and the thin outer wall of the flared end (metaphysis). Trabecular bone is continuous with the inner surface of the cortex and exists as a three-dimensional lattice of bony plates and columns (trabeculae). The trabeculae divide the interior volume of the bone into intercommunicating pores, which are filled with a variable mixture of red and yellow marrow. The characteristic dimensions of the pores vary considerably throughout the bone interior, resulting in a structure of variable density (*1*).

The differences in morphology and mechanical behavior of compact and trabecular bone have prompted many researchers to investigate these two bone types as if they were different materials (*2*). Recently, however, some workers have attempted to view trabecular bone as a porous structure comprised of bone tissue with the same microscopic mechanical properties as compact bone (*3–8*). The purpose of the study reported here was to further explore the hypothesis that all bone can be mechanically viewed as a single material. We were also interested in deriving a simple expression to describe the compressive strength of all bone as a function of apparent density and the applied strain rate.

In order to determine the compressive strength of trabecular bone spanning a large density range, we examined both human and bovine bone. In addition to specimen density, the effect of strain rate and the effect of marrow in situ were examined. Specimens of compact bone were not tested since there are adequate data on the mechanical properties of compact bone in the literature. One hundred cylindrical specimens of human trabecular bone and 24 specimens of bovine trabecular bone were machined under continuous irrigation. The specimens were 5 mm thick and 10.3 mm in radius, were removed from human tibial plateaus and bovine femoral condyles, and were oriented with their axes paral-

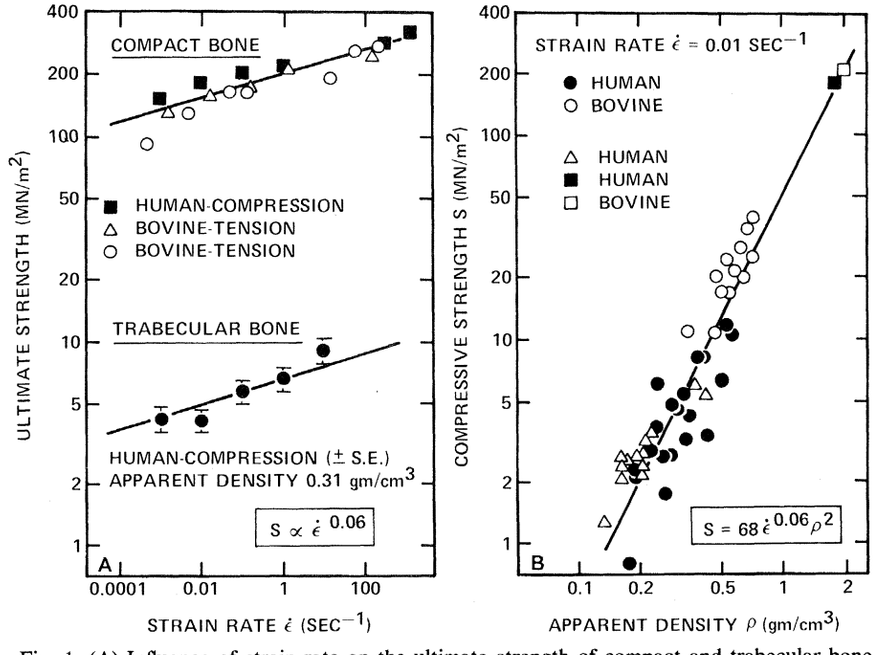

Fig. 1. (A) Influence of strain rate on the ultimate strength of compact and trabecular bone tested without marrow in situ. Data denoted by filled circles are from this study (± S.E.), filled squares are from (*11*), open triangles from (*12*), and open circles from (*13*). (B) Influence of apparent density on the compressive strength of trabecular and compact bone. Data denoted by filled and open circles are from this study, open triangles are from (*10*), filled and open squares from (*11*).

lel to the long axis of the bone. After machining, the specimens were stored at −20°C until testing (*9*). A random allocation scheme was used to divide the specimens into 12 test groups. Half of the human specimens and all the bovine specimens were tested after the marrow was removed with an air jet and running water. Specimens were tested in uniaxial strain by confining them in a rigid cylindrical cavity and compressing them by more than 50 percent of the original thickness in an electrohydraulic materials testing machine (MTS Systems). Porous compression platens with a nominal pore size of 165 μm allowed for the escape of marrow from the specimens.

After testing, the marrow was extracted from the specimens tested with marrow in situ. All of the specimens were then degreased with ethanol. After vacuum degassing, the specimens were weighed while immersed in distilled water to determine the submerged weight. Specimens were then centrifuged at 8000*g* for 15 minutes to remove residual water from the pores and weighed in air to determine the wet weight. The volume of bone tissue (excluding pores) was calculated as the difference between wet and submerged weight (*10*). Specimen tissue density was found by dividing wet weight by bone tissue volume, and specimen apparent density by dividing wet weight by initial specimen volume as measured with a micrometer. Although the apparent densities varied from 0.07 to 0.97 g/cm^3, the tissue densities were approximately equal to that of compact bone (1.6 to 2.0 g/cm^3).

Viscous flow of marrow out of the pores led to strengthening of the bone only in the ten specimens tested with marrow at the highest loading rate (strain rate $\dot{\epsilon} = 10$ sec^{-1}). When these specimens were eliminated from consideration, the loading rate effect on compressive strength was found to be similar to that previously reported for compact bone (*11–13*). Figure 1A shows a linear log-log relationship between ultimate strength and strain rate for compact bone as well as for the human trabecular bone specimens of this investigation. The data for the trabecular bone were adjusted to the specimens' mean apparent density of 0.31 g/cm^3 by using power curve fits for the data at each strain rate. The data of Fig. 1A are consistent with the hypothesis that the slopes of both curves are equal to 0.06. We suggest, therefore, that the compressive strength of bone tissue is approximately proportional to the strain rate raised to the 0.06 power. This power law relationship between bone compressive strength and strain rate is consistent with experimental results for plastic foams. Hinckley and Yang (*14*) conducted compression tests of rigid polyurethane foams of three different densities over five decades of strain rate. When their data are replotted on log-log scales, a relationship analogous to that shown by bone in Fig. 1A results.

The effect of specimen apparent density on compressive strength at a strain rate of 0.01 sec^{-1} is shown in Fig. 1B. In addition to the results for the specimens of this investigation, other data for trabecular (*10*) and compact (*11*) bone are shown. On a log-log plot, all the data are well described by a straight line with a slope of 2.0. These results suggest that the compressive strength of bone is proportional to the square of the apparent density. This power law relationship between compressive strength and apparent density is also consistent with theoretical and experimental work on rigid cellular plastics (*15*). The basic assumption of the theoretical explanation for the squared relationship is that the cellular struts (trabeculae in the case of bone) fail by buckling. Previous work on trabecular bone suggests that buckling is indeed a major failure mode (*8, 16–18*).

The results of this investigation suggest that the longitudinal compressive strength of bone can be described by the equation

$$S = S_c\dot{\epsilon}^{0.06}\left(\frac{\rho}{\rho_c}\right)^2 \qquad (1)$$

where S is the compressive strength [meganewton (MN)/m^2] of a bone specimen of apparent density ρ (g/cm^3) tested at a strain rate of $\dot{\epsilon}$ (sec^{-1}) and S_c is the compressive strength (MN/m^2) of compact bone with a density of ρ_c (g/cm^3) tested at a strain rate of 1.0 sec^{-1}. Human compact bone tested at a strain rate of 1.0 sec^{-1} has a compressive strength of 221 MN/m^2 (*11*) and a density of approximately 1.8 g/cm^3 (*19*). Using these values, we simplify Eq. 1 to

$$S = 68\dot{\epsilon}^{0.06}\rho^2 \qquad (2)$$

Equation 2 shows that compressive strength is a strong function of the specimen apparent density and a weak function of the imposed strain rate. This expression is most useful in describing strength changes when large density variations are present. A more rigorous analysis accounting for factors such as bone ultrastructure, mineralization, trabecular orientation, and disease state is needed to more exactly describe the compressive behavior of bone over a narrow range of density.

The results of this investigation provide clinical guidelines for predicting bone strength in patients with decreased skeletal mass. Rarefaction of bone (osteoporosis) is present in many pathological conditions and is a common finding in bedridden or elderly patients. In all types of osteoporosis, the earliest and most striking change is in trabecular bone, where the trabeculae become thin and sparse (*20*). Later clinical features may include compressed vertebral bodies, chronic back pain, dorsal kyphosis (hunched back), and general skeletal pain. Gross pathological fractures including fractures of the femoral neck are further clinical complications (*20, 21*).

Recent advances in the development of densitometric techniques have made it possible to clinically monitor the distribution of bone density and the loss of skeletal mass (*22–24*). For example, photon absorption densitometry studies have shown that the ulnar bone densities in osteoporotic patients may be reduced to as little as one-third of normal (*25*). The results of this investigation suggest that in these patients the bone compressive strength is reduced to one-ninth of normal. The observed increase in the incidence of ulnar crush fractures in osteoporotic patients (*25*) is consistent with this predicted reduction in strength.

In conclusion, our findings support the hypothesis that all bone can be mechanically viewed as a single material of variable density. The results of this investigation also enable the clinician to make meaningful predictions of bone strength based on in vivo density measurements.

DENNIS R. CARTER
Department of Orthopaedics, University of Washington School of Medicine, Seattle 98195
WILSON C. HAYES
Department of Orthopaedic Surgery, University of Pennsylvania School of Medicine, Philadelphia 19174

References and Notes

1. E. D. Dyson, C. K. Jackson, W. J. Whitehouse, *Nature (London)* **225**, 957 (1970).
2. F. G. Evans, *Mechanical Properties of Bone* (Thomas, Springfield, Ill., 1973).
3. J. H. McElhaney, N. M. Alem, V. L. Roberts, *ASME Publ. 70-WA/BHF-2* (1970).
4. R. B. Martin, *J. Biomech.* **5**, 447 (1972).
5. J. W. Pugh, R. M. Rose, E. L. Radin, *ibid.* **6**, 657 (1973).
6. J. W. Pugh, R. M. Rose, I. L. Paul, E. L. Radin, *Science* **181**, 271 (1973).
7. J. Black, *ibid.*, p. 273.
8. P. R. Townsend, R. M. Rose, E. L. Radin, *J. Biomech.* **8**, 199 (1975).
9. E. D. Sedlin and C. Hirch, *Acta Orthop. Scand.* **37**, 29 (1966).
10. J. Galante, W. Rostoker, R. D. Ray, *Calcif. Tissue Res.* **5**, 236 (1970).
11. J. H. McElhaney and E. F. Byars, *ASME Publ. 65-WA/HUF-9* (1965).
12. R. D. Crowninshield and M. H. Pope, *Ann. Biomed. Eng.* **2**, 217 (1974).
13. T. M. Wright and W. C. Hayes, *Med. Biol. Eng.*, in press.
14. W. M. Hinckley and J. C. S. Yang, *Exp. Mech.* **15**, 177 (1975).
15. M. R. Patel, thesis, University of California, Berkeley (1969).

16. G. H. Bell, *Adv. Sci.* **26**, 75 (1969).
17. J. W. Pugh, R. M. Rose, E. L. Radin, *J. Biomech.* **6**, 475 (1973).
18. W. C. Hayes and D. R. Carter, paper presented at the 7th Annual International Biomaterials Symposium, Clemson, S.C. (1975).
19. O. Lindahl and A. G. H. Lindgren, *Acta Orthop. Scand.* **39**, 129 (1968).
20. R. B. Salter, *Textbook of Disorders and Injuries of the Human Musculoskeletal System* (Williams & Wilkins, Baltimore, 1970), pp. 137–138.
21. M. V. L. Foss and P. D. Byers, *Ann. Rheum. Dis.* **31**, 259 (1972).
22. J. R. Cameron and J. A. Sorenson, *Science* **142**, 230 (1963).
23. R. B. Mazess, J. R. Cameron, R. O'Connor, D. Knutzen, *ibid.* **145**, 388 (1964).
24. D. H. Kranendonk, J. M. Jurist, H. G. Lee, *J. Bone J. Surg. Am. Vol.* **54**, 1472 (1972).
25. B. E. C. Nordin *et al.*, in *Osteoporosis*, U. S. Barzell, Ed. (Grune and Stratton, New York, 1970), pp. 47–67.
26. We thank A. Leach for assistance in specimen preparation. Supported by the National Institutes of Health under grant NIH-1R01-AM-18376-01 and the National Science Foundation through the Center for Materials Research, Stanford University.

18 June 1976

Presynaptic Facilitation as a Mechanism for Behavioral Sensitization in *Aplysia*

Abstract. *Sensitization is an elementary form of nonassociative learning, related to behavioral arousal, in which a strong stimulus facilitates a reflex response. Studies of the neural circuit of the gill-withdrawal reflex in the isolated abdominal ganglion of* Aplysia *indicate that short-term sensitization is due to presynaptic facilitation. The facilitation results in a sudden increase in the amount of neurotransmitter released by the sensory neurons at their synapses with motor neurons.*

The ability to study behavior on a cellular level in a number of higher invertebrates (*1*) makes is possible to examine the cellular and synaptic alterations produced by simple forms of behavioral modifications and to begin to explore their molecular mechanisms. This report and its companion (*1a*) represent an attempt to apply this approach in *Aplysia*.

Sensitization is an elementary form of learning in which a strong or noxious stimulus enhances an animal's preexisting reflex responses for periods ranging from minutes to several weeks, depending upon the pattern and duration of training (*2*). Sensitization resembles classical conditioning in that activity in one pathway facilitates reflex activity in another. Unlike classical conditioning, however, reflex facilitation does not require specific temporal association of the two stimuli. As a result of this similarity to classical conditioning, sensitization is thought by some to be closely related to associative learning (*3*). Sensitization can also produce dishabituation, the enhancement of a reflex response that has previously been habituated (*4, 5*). Whereas habituation is restricted to the stimulated pathway, sensitization alters the responsiveness of a variety of related reflex pathways. Because both sensitization and behavioral arousal lead to increased responsiveness that is generalized and sustained, sensitization is thought to be a component of behavioral arousal (*5, 6*).

We have studied the cellular mechanisms underlying sensitization of the gill-withdrawal reflex in the marine mollusk *Aplysia*. Our results indicate that sensitization involves a novel synaptic mechanism, presynaptic facilitation.

Weak or moderate stimulation of the siphon leads to brisk withdrawal of the gill. A single training session of 10 to 15 repeated stimuli results in short-term habituation (15 minutes to several hours) of the reflex response. The reflex response can be abruptly enhanced for many minutes if a single strong sensitizing stimulus is applied to the head (*2*).

The neuronal mechanisms of short-term habituation and sensitization can be studied in the isolated abdominal ganglion (Fig. 1A). The ganglion contains an identified cluster of 24 sensory neurons that innervate the siphon skin and 6 identified motor neurons that mediate the gill-withdrawal reflex (*7*). The sensory neurons make direct monosynaptic excitatory connections with the motor neurons (*8, 9*). With repeated sensory stimulation at rates that produce habituation in the intact animal (once every 10 seconds to once every 3 minutes), the monosynaptic excitatory postsynaptic potential (EPSP) produced in the motor neuron by action potentials in the sensory neuron becomes depressed (Fig. 1B) due to a decrease in transmitter release by the sensory neuron (*9*). Electrical stimulation (6 hertz for 10 seconds) of the neural pathway (connective) from the head ganglion that mediates the effect of a sensitizing stimulus in an intact animal rapidly facilitates the EPSP for about 50 minutes (Fig. 1, B and C) [for a similar phenomenon in another synaptic system in *Aplysia*, see (*10*)]. The facilitating stimulus does not fire the sensory neuron (Fig. 1B); this distinguishes this form of heterosynaptic facilitation from posttetanic facilitation resulting from repetitive activity in the sensory neurons (*5, 10*).

To determine whether the facilitation occurs presynaptically or postsynaptically, we have used a quantal analysis. This analysis is technically difficult to achieve in most central neurons because they receive many synaptic in-

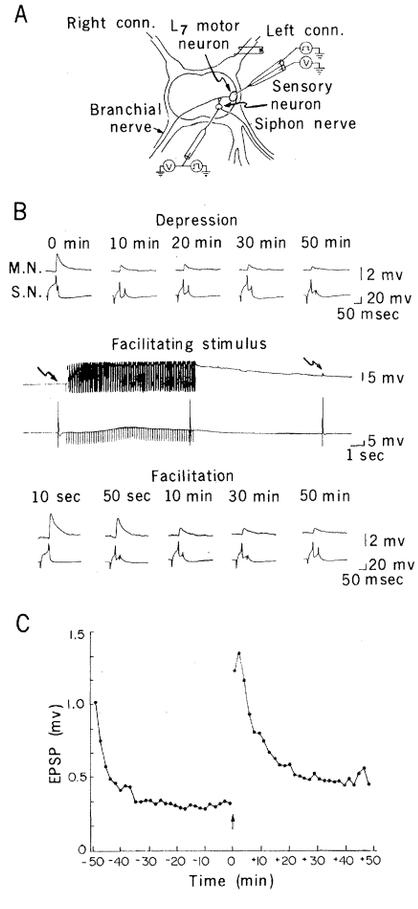

Fig. 1. Synaptic facilitation at the synapse between mechanoreceptor neurons and motor neurons. (A) Ventral aspect of the abdominal ganglion of *Aplysia* illustrating simultaneous recording from gill motor neuron L_7 and a mechanoreceptor sensory neuron. (B) Depression and subsequent facilitation of a monosynaptic EPSP after a strong stimulus. Arrows indicate the last EPSP before the facilitating stimulus and the first EPSP after the stimulus. Abbreviations: *S.N.*, sensory neuron; *M.N.*, motor neuron. (C) Time course of facilitation. Data were obtained from an experiment similar to the one illustrated in (B). Each point represents the average amplitude of ten successive evoked EPSP's. Facilitation occurred at time 0, when the left connective was stimulated as in (B). The EPSP's are facilitated beyond the initial control amplitude. We do not know to what extent the decline after the facilitating stimulation is due to continued testing or to gradual spontaneous recovery from facilitation.